



## Assessing vertical structure of an endemic forest in succession using terrestrial laser scanning (TLS). Case study: Guadalupe Island

Fabiola D. Yépez-Rincón<sup>a,d,\*</sup>, Luciana Luna-Mendoza<sup>b</sup>, Nelly L. Ramírez-Serrato<sup>d,e</sup>,  
Alejandro Hinojosa-Corona<sup>c</sup>, Adrián L. Ferriño-Fierro<sup>a</sup>

<sup>a</sup> Universidad Autónoma de Nuevo León, Mexico

<sup>b</sup> Grupo de Ecología y Conservación de Islas, A.C., Mexico

<sup>c</sup> Centro de Investigación Científica y de Educación Superior de Ensenada, Mexico

<sup>d</sup> Teebcon Servicios Ingenierías y Proyectos, SA de CV, Mexico

<sup>e</sup> Universidad Nacional Autónoma de, Mexico

### ARTICLE INFO

Editor: Jing M. Chen

#### Keywords:

Management plan assessment

Remote sensing

Vegetation indexes

Guadalupe Island

### ABSTRACT

Endemic species comprise 16% of the floral species on Guadalupe Island, including three arboreal species. Almost 96% of the forest coverage was lost due to impacts related to feral goats and wildfires. To date, goats have been eradicated and the restoration of the native vegetation communities is underway. The purpose of this study was to develop a 3D Structural Classification Method (3D-SCM) using Terrestrial Laser Scanner (TLS) for mapping the vertical structure of the forest and to automatically characterize its physical attributes. Several TLS scans were performed in July 2016 to assess this recovery, particularly the succession progression. The 3D-SCM used the Forest Condition Classification (FCC) based on radiometric intensity and height values, and the Individual Shape Index (ISI) based on geometry and intensity parameters. It was designed to classify vegetation by stratum using a trial-and-error model to semi-automatically identify impacted areas and succession. The 3D-SCM was able to differentiate the vegetation strata by each forest community at the stand level with a precision of 93% as well as the tree structure parts (stem, branches, and leaves) with a precision of 97%, it also fits the best characteristic shape for the Guadalupe cypress (decagon) and for the pine (droplet). The resulting 3D-SCM provide precise physical specifications, demonstrates a high correlation  $R^2 = 0.949$  for (Diameter Breast Height) DBH,  $R^2 = 0.974$  for the crown and  $R^2 = 0.97$  for heights between maximum laser pulse of tree heights and crowns with respect to field measurements. Mapping 3D vertical forest measurements are important for quantifying the success of management practices and to assist future restoration actions, as it will allow quantification of forest dynamics and carbon sequestration on this island.

### 1. Introduction

Guadalupe Island is the fifth largest (24,171 ha) Mexican island located in the Pacific Ocean 260 km from the Baja California Peninsula (Fig. 1A). It has a maximum elevation of 1298 m (García-Gutiérrez et al., 2005; Ramírez Serrato, 2014). The island and surrounding waters were declared a Biosphere Reserve in 2005 (CONANP, 2013). Feral goats were introduced to Guadalupe Island in the 19th century by sealers from England, Russia and North America (Aguirre-Muñoz et al., 2011; Moran, 1996). A century later, the feral goats had dramatically changed all native vegetation communities. In 2007 goats were eradicated from the

island, allowing the vegetation to recover. When trees or the understory are removed, the forest regenerates in a predictable order (Oliver, 1980). First annual weeds appear, then perennial weeds and grasses, followed by shrubs and coniferous trees (O'Hara et al., 1996). Each stage of succession has its own vertical structure and provides different benefits to a variety of wildlife species.

The Guadalupe Island cypress (*Cupressus guadalupensis*) is an endemic forest. This environment has experienced different treatments, starting with the intense overgrazing of feral goats, then the almost total elimination of its adult forest through wildfires. Its subsequent recovery presented a demographic explosion of cypress shoots, which are now

\* Corresponding author at: Universidad Autónoma de Nuevo León, Mexico.

E-mail addresses: [fabiola.yepzrn@uanl.edu.mx](mailto:fabiola.yepzrn@uanl.edu.mx) (F.D. Yépez-Rincón), [luciana.luna@islas.org.mx](mailto:luciana.luna@islas.org.mx) (L. Luna-Mendoza), [nellyrmz@igeofisica.unam.mx](mailto:nellyrmz@igeofisica.unam.mx) (N.L. Ramírez-Serrato), [alhinc@cicese.mx](mailto:alhinc@cicese.mx) (A. Hinojosa-Corona), [adrian.ferrinofr@uanl.edu.mx](mailto:adrian.ferrinofr@uanl.edu.mx) (A.L. Ferriño-Fierro).

<https://doi.org/10.1016/j.rse.2021.112563>

Received 17 July 2020; Received in revised form 17 May 2021; Accepted 12 June 2021

Available online 30 June 2021

0034-4257/© 2021 The Authors. Published by Elsevier Inc. This is an open access article under the CC BY license (<http://creativecommons.org/licenses/by/4.0/>).

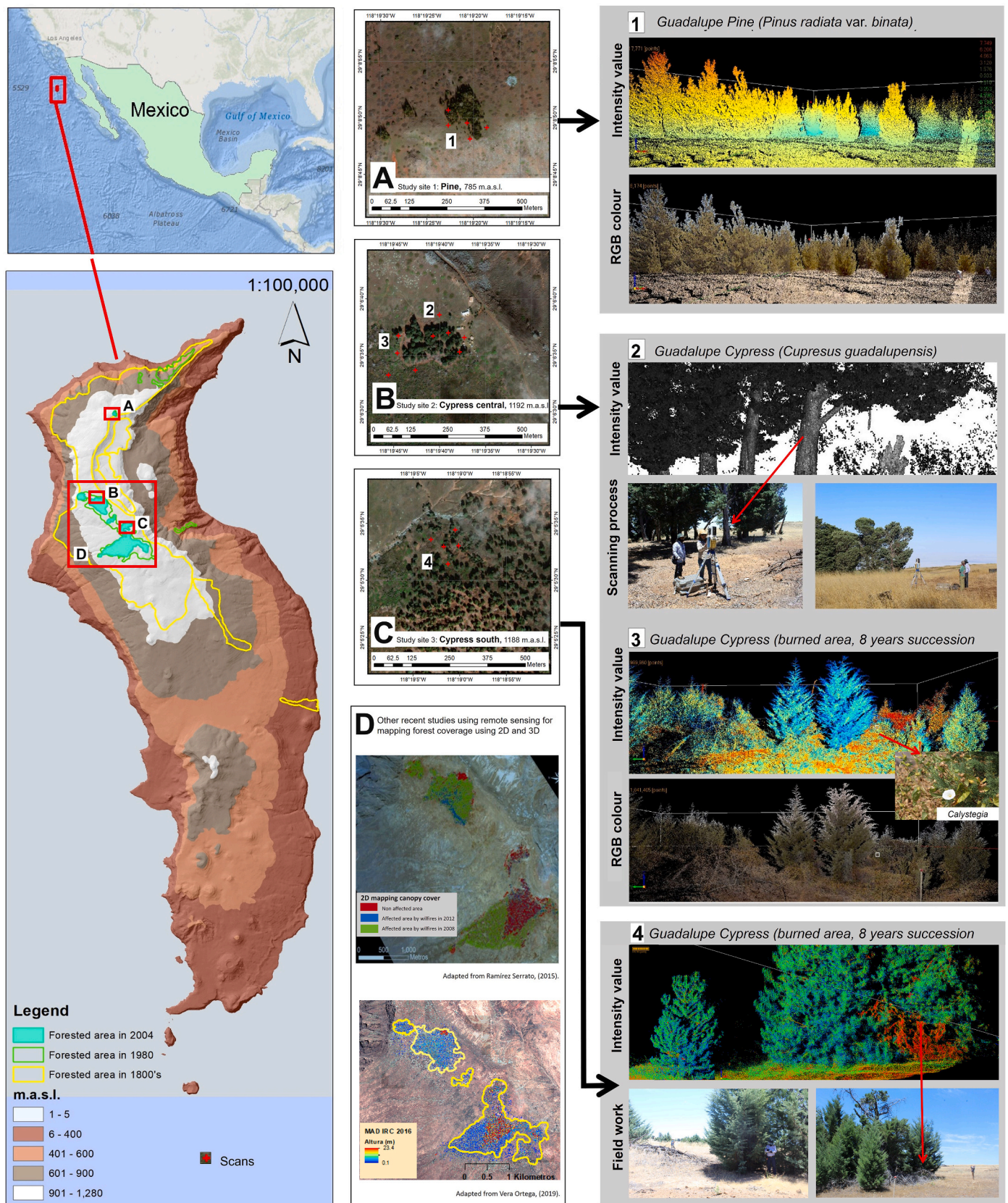


**Fig. 1.** (Left to right) Guadalupe Island location; A site, is the northern patch with pine forest (pine site); B site is within the cypress forest (cypress central site); C site is inside the cypress forest (cypress south site); 1, 2 and 3 are examples of scanning processes and their locations; D (upper) shows in red the areas of the cypress forest not affected by the 2008 fire, and in green burned areas; D (lower) is a canopy height model derived from 2016 UAV NIR (near infrared) photogrammetry. (For interpretation of the references to colour in this figure legend, the reader is referred to the web version of this article.)

juvenile trees mixed with secondary species that make up the different stages of succession in this ecosystem. Because this is an endemic forest in a critical situation, it is important to characterize its attributes and determine the physical and spatial properties of the species that comprise it, which will provide data for future monitoring and conservation studies of the area. The assessment of the 3D vertical structure of the Guadalupe Island forest through the digitalization of their physical attributes may improve measurement data to better understand the succession of its ecosystem processes.

Through remote sensing images forest succession can be assessed (Falkowski et al., 2009). In addition to 2D images, laser-based techniques have been also used, in both Terrestrial Laser Scanner (TLS) or Aerial Laser Scanner (ALS) modes. These permitted experimentation with 3D work scales at the individual level which were focused on obtaining forest parameters for estimating biomass such as the tree height and mean crown width (Wan Mohd Jaafar et al., 2018), as well as basal area (m<sup>2</sup>), and stem volume (m<sup>3</sup>) attributes (Silva et al., 2016). Non-parametric methods such as canopy height model (CHM), Random Forest k-nearest neighbor (RF k-NN) and FUSION have been developed for this type of studies (McGaughey et al., 2004). The characterization of the different strata of a forest in succession by laser technology has been used (Szostak, 2020) to monitor plantations (Kolecka, 2018) and support projection of fauna behavior (Rechsteiner et al., 2017).

## 2. Background

### 2.1. Impacts: Feral goats and wildfires

Feral goats caused the extinction and extirpation of more than 30 species of plants (Moran, 1996) with resulting loss of habitat for the native fauna (Jehl and Everett, 1985). There have been several fires recorded on Guadalupe Island in the last four decades, at least three in the cypress forest and one in the pine forest (Melling, 1985). In 2008, shortly after the goats were eradicated, a fire occurred in the forest. Massive seed release and sapling recruitment occur post-fire, the most recent example resulting from a fire in the endemic cypress forest (de Gouvenain and Ansary, 2006; Oberbauer et al., 2009; Rodríguez-Buriticá and Suding, 2013). Endemic species from the understory such as *Ceanothus arboreus* and *Arctostaphylos* sp., could benefit from fire since both species were found in the forest after the fire. The low intensity 2008 fire resulted in high mortality of existing cypress trees due to exposure of heartwood from damage encountered from the feral goat population. Post-fire assessment describes a robust regeneration due to serotiny of cypress cones in addition to accelerated vegetation recovery of multiple species as a result of the fire (Oberbauer et al., 2009).

### 2.2. Forests on Guadalupe Island

#### 2.2.1. Pine forest

Historically, the endemic Guadalupe Monterey Pine forest (*Pinus radiata* var. *binata*), located in the northern part of the island (Fig. 1A), covered 2400 ha (Oberbauer, 2005). Due to the impacts by feral goats, this coverage decreased drastically. In 2001 it was estimated that 220 pines survived (Rogers et al., 2006), and the chaparral component was virtually absent. Maritime scrub remained with few individuals of several species surviving on cliffs and a few survivors of the chaparral were able to subsist as part of the seedbank (Luna-Mendoza et al., 2019). After the goat eradication, the forest started to recover. New seedlings of pines, together with native shrub, scrub and forb species are thriving (Aguirre-Muñoz et al., 2011).

#### 2.2.2. Cypress forest

Similar to the pine forest, the original coverage of the Guadalupe cypress was dramatically reduced after goat introduction (Greene, 1885; Moran, 1996). Cypress could have been distributed in the entire plain of the northern end of the island, together with chaparral and maritime

scrub prior to goat introduction (Moran, 1996). By the end of the 1800's the cypress forest coverage in the island was estimated between 520 and 780 ha (Franceschi, 1893) and by 2004 the coverage was reduced to 160 ha (Fig. 1B and C) (Garcillán et al., 2009; Oberbauer et al., 2009; Oberbauer, 2005). Only adult trees survived, and no recruitment was recorded for more than a century. The unburned part of the forest is dominated by old cypress and some annual weeds (such as European grasses).

#### 2.2.3. Secondary vegetation and succession process

After a wildfire in Guadalupe Island the appearance of secondary vegetation occurs. The burned area has restarted its gestational stage until it becomes a forest in succession. This is the process by which a forest can naturally revive to adulthood. The forest floor was exposed after the fire, which caused some annual shrub species to take advantage of the space. These species require less care, they can withstand the sun that now enters directly, the lack of nutrients, water, and high temperatures. Over time, the seeds that were sown from the cypress tree began to develop but this time taking advantage of the microclimate created by the shrub species. The contrast between burned and secondary non-burned forest, withstanding juvenile cypress (new recruits), was an abundance of previously threatened species: *Calystegia macrostegia* (*macrostegia*); *Ceanothus* (*Ceanothus* sp.) And Large-leafed lotus (*Acmispon grandiflorus*) correspond to this secondary vegetation, which at the moment is coexisting and protecting the sprouts of Cypress trees (Garcillán et al., 2009).

### 2.3. Mapping forest recovery on Guadalupe Island

To evaluate historical changes and recovery, the cypress forest of the island has been mapped to estimate its coverage at different periods using high resolution satellite imagery (WorldView 2, QuickBird and FireMapper sensors) (Ramírez Serrato, 2014; Rodríguez-Malagón, 2006). Changes of the cypress forest were analyzed using NDVI (Normalized Difference Vegetation Index) and TSAVI (Transformed Soil Adjusted Vegetation Index) during an 8-year period (2004 to 2012). An increment of 27% of secondary vegetation cover was recorded (Fig. 1D) (Ramírez Serrato, 2014). Vera-Ortega (2019) used Unmanned Aerial Vehicles with RGB and Near-Infrared cameras to map ~600 ha of cypress forest on the island in 2016 and 2019. Ultra-high resolution orthoimages and photogrammetrically derived point clouds were produced to obtain canopy height models (CHM) for the cypress forest. This work (Vera-Ortega, 2019) found that juvenile cypresses from the recovering areas are growing in coverage and volume, but adult trees are dying or losing important canopy densities.

A more detailed study of the vertical structure or 3D mapping with TLS data was needed to understand the ecological succession of the forest after a long history of impacts as well as the restoration actions. The vertical structure of the canopy is recognized as “the spatiotemporal organization that includes position, extension, density, type and connectivity of the vegetation components on the ground” (Parker, 1995). Characterization of the canopy structure is an important key factor to quantify forest resources (Nelson et al., 1988; Parker, 1995), as well as essential to understand the availability of refuge, food, and other habitat conditions for wildlife (Bergen et al., 2007; Hansen and Rotella, 2000; Hyde et al., 2006) and to comprehend the ecosystems processes and functions (Cramer et al., 2001; Gower et al., 1999; Hansen and Rotella, 2000; Lefsky et al., 1999).

### 2.4. Assessment of vertical forest structure using terrestrial laser scanning (TLS)

Laser altimeters have been used to estimate canopy heights since the 80's (Aldred and Bonnor, 1985; Nelson et al., 1988); with greater precision than through manual data collection or mapping the canopy coverage changes with forest scans (Maclean and Krabill, 1986;

**Table 1**  
Configuration of the GLS-1500 laser scanner in Normal mode.

Parameters	Characteristics
Maximum range 90% reflectivity	330 m
Maximum range 18% reflectivity	150 m
Scanning mechanism	Rotating/oscillating
Single point accuracy (distance at 1 to 150 m)	4 mm
Scan rate	30,000 points per second
Laser type	Pulsed (time of flight)
Wavelength	1535 nm (invisible, eye-safe)
Intensity recording (digital number)	From 1 to 3500
Laser class	1

Magnusson et al., 1999). TLS is an active sensor capable of producing 3D information of the scanned targets making it a promising tool for mapping the vertical structure of vegetation with fine detail (Guo and Feng, 2020; Schneider et al., 2019). It has been used since 2006 (Estornell et al., 2012; Hopkinson et al., 2004) to estimate vegetation biomass (Calders et al., 2015), forest metrics (Hopkinson et al., 2004), and topography on wooded land (Kraus and Pfeifer, 1998). Only recently 3D forest structure data, obtained with TLS, have been used for the direct measurement of forest parameters (Rowell et al., 2020; Yubo et al., 2019).

TLS emits laser pulses at high rates and registers the beam echoes on the receiver, obtaining, in addition to the spatial information, other values such as the reflectivity of the object or intensity. These intensity values use the function of the near infrared spectral band (Lang and McCarty, 2009) (Table 1), and the number of returns per pulse. Point clouds produced by the scanners allow the identification of forest strata when there are good quality and high-density data (Van Leeuwen and Nieuwenhuis, 2010). A dense point cloud is useful for quantifying

volume and other forest attributes (Popescu et al., 2004). Consequently, TLS data are increasingly being used for ecological studies (Lefsky et al., 1999) and habitat modeling (Goetz et al., 2007; Streutker and Glenn, 2006; Vierling et al., 2008). A dense point cloud can be used to automate measurements that ecologists often do manually and qualitatively. The precise digital representation of the real world could help to more accurately quantify an environment which is always changing.

TLS has been used to automate vertical vegetation measures with a single scan. Research has focused on correcting scan errors with the use of other sources such as ALS (Calders et al., 2014). TLS has primarily been applied to retrieve forest inventory variables from above-ground biomass (Disney et al., 2019; Maas et al., 2008) including diameter at breast height, tree height (Watt and Donoghue, 2005), crown variables (Jung et al., 2011), basal area and volume (Moskal and Zheng, 2012). These variables can be used for assessing the potential of wildfire hazard (Fernandes, 2009). Other forest variables assessed include overall density, vertical structure, and competitive conditions for regeneration, horizontal visibility, and three-dimensional structural variability. This information can be used to implement management practices (Seidel et al., 2016) as well as study temporal change (Kaasalainen et al., 2014; Liang et al., 2012; Srinivasan et al., 2014). Applications of TLS range from retrieval of traditional parameters of forest structure such as stem breast diameter and tree height (Maas et al., 2008), to quantitative descriptions of the tree components (branches, trunk, etc.).

Many vegetation classification methods are based on geometric characteristics (Wang et al., 2020), on radiometric intensity limits (Cruz et al., 2012) or the combination of both (Zhu et al., 2018). Intensity-based methods are built on the assumption that leaves and wood components have different optical properties at the operating wavelength of the laser scanner (Tao et al., 2015). However, such properties are generally influenced by distance, a laser impact, and its angle of

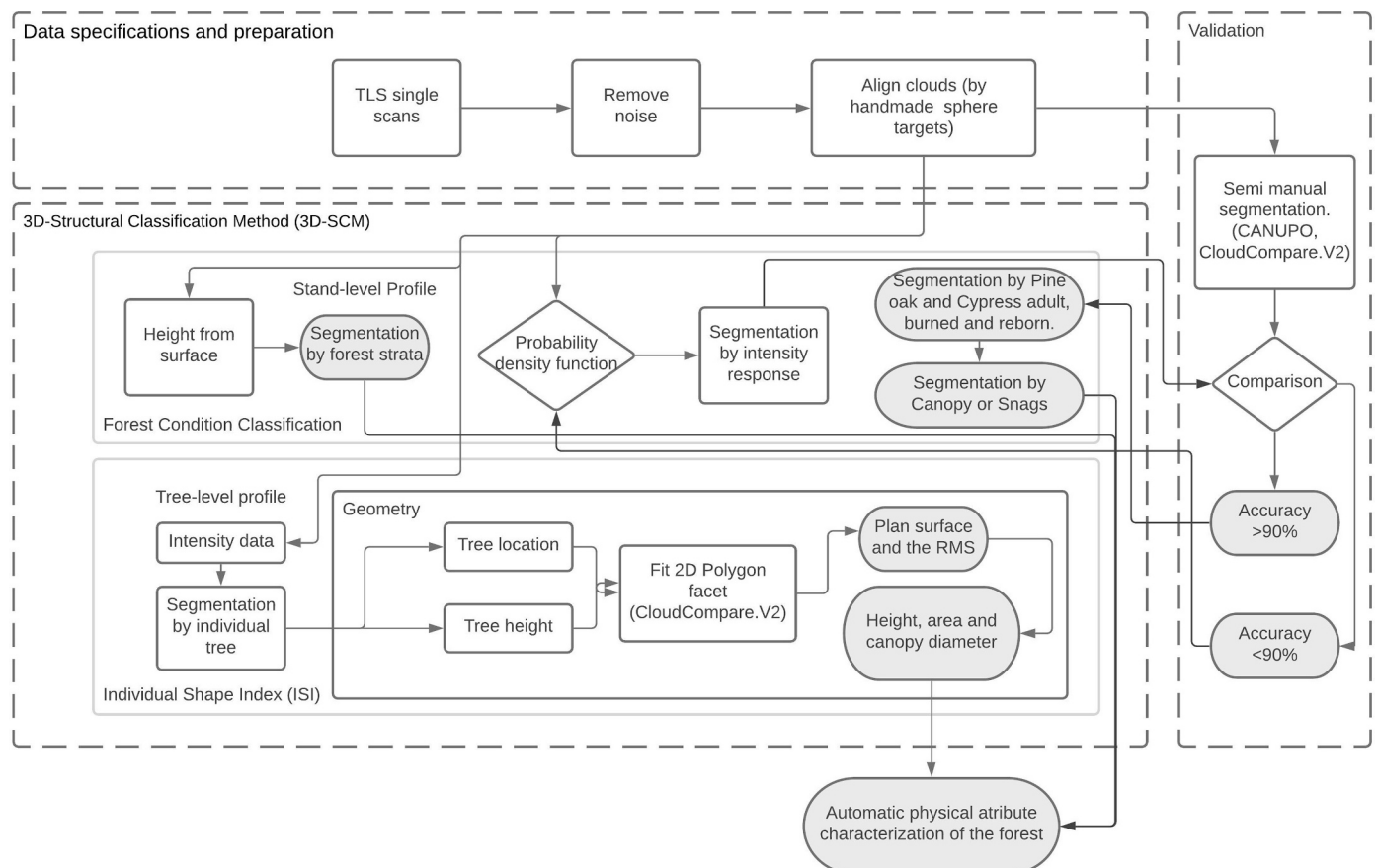


**Fig. 2.** The workflow specifies data usage and preparation the 3D Structural Classification Method and validation process.

incidence (Singh et al., 2020).

Segmentation studies using TLS point clouds have been carried out with the creation of software for specific segmentation for this type of inputs (Hackenberg et al., 2015), and even comparisons between segmentation algorithms (Bournez et al., 2017). However, each of these algorithms is based on specific shapes of the region used, such as cone-shaped pines (Li et al., 2012), so each forest has different measurements and dimensions. Each of these algorithms is based on old forests, where most of the coverage corresponds to adult trees of similar species. The purpose of this study is to obtain the specific properties to calibrate segmentation algorithms for two old forests of adult cypress pine and Monterrey pine trees, as well as considering a forest in succession of at least four vegetation horizons.

The novel approach presented in this paper is the design and evaluation of a classification method for 3D mapping of the vertical structural composition of pine and cypress forests. The method proposed in this study may improve future assessments to fully understand the succession ecosystem processes of these endemic forests and can inform future management and conservation practices.

## 2.5. Objective

Considering the uniqueness and critical situation of the Guadalupe Island forest, the objective of this study was to develop and evaluate a methodology that characterizes the tree succession using intensity thresholds, intervals of heights above the ground and geometric characteristics for individual trees and canopy layers.

## 3. Materials and methods

3D Structural Classification Method (3D-SCM) is an innovative method to map canopy layers and tree vertical structure (stem, branches, and leaves) designed and tested to monitor the success of forest management practices. This robust methodology uses Terrestrial Laser Scanner (TLS) to assess the vertical stand structure from the forests at Guadalupe Island. The general workflow of 3D-SCM is displayed in Fig. 2 following 3 stages: (a) Data specifications and preparation, (b) 3D-SCM development and assessment, based on the Forest Condition Classification (FCC) and the Individual Shape Index (ISI), and (c) Validation process. The process combines semi-automatic algorithms used to classify the point clouds based on variables such as intensity thresholds, above ground heights and geometry characteristics to classify the forest canopy layers. Once these variables are mapped, a manual selection of tree architecture classes was used (to trial-and-error) to adjust the automatic filters in the algorithm to improve accuracy.

### 3.1. Study sites

TLS scanning was done on three sites of interest: Northern (pine forest; Fig. 1A), Central (cypress forest) and Southern (cypress forest) sites (Fig. 1B and C, respectively).

#### 3.1.1. Pine

The pine site (Fig. 1A) is located over the crest of the highest peaks at the north of the island. This site is a patch located in the southern limit of the pine forest. It comprises nine adult trees, several thousands of juvenile trees, and some native shrubs. European grasses and native and non-native forbs are abundant.

#### 3.1.2. Cypress central

Before the 2008 fire, the cypress forest comprised three main patches of adult trees: north, central, and south (Rodríguez-Malagón, 2006). After the fire only the last two had adult trees, the north patch is now composed of juvenile cypress, no adults survived. The cypress central patch (Fig. 1B) is at the northern limits of the cypress adult forest distribution. A biological station is located nearby, surrounded by adult

trees which were not affected by the 2008 fire. The rest of the patch was severely affected by fire and now has thousands of cypress saplings, secondary vegetation and remaining standing dead (burned) trees or snags, and branches of adult cypress. This sampling site was divided in two sections: unburned and burned areas.

#### 3.1.3. Cypress south

Cypress south is the largest cypress patch remaining. The tree density is lower compared to other patches, and it was less affected by the 2008 fire (Fig. 1C). This patch is divided in the northeast area composed by adult and juvenile cypress, which was not affected by the fire, and the southwest area with juvenile cypress and secondary vegetation but in lower densities than in the burned area of the cypress central patch.

## 3.2. Terrestrial laser scanner (TLS)

A GLS-1500 terrestrial laser scanner (Topcon Co., Japan), with technical configuration in the Normal Mode (Table 1) was used to obtain dense point clouds. The maximum measurable range of the scanner is 500 m (for target objects with 90% reflectance), and it can achieve 4 mm accuracy at a 150 m range and 6° of angle (H&V). The minimum point spacing is 1 mm at 20 m distance; spot diameter of laser is approximately 16 mm at 100 m. For this study, the distance was set to 70 m. The device uses an infrared laser with a wavelength of 1535 nm (Class 1 laser, invisible, eye safe). Scan rate is up to 30,000 points per second, while the time for one scanning operation at a given position was approximately 30–60 min, including set up, object scanning, target marker measurement unit and photograph (RGB colour) capture. The complete equipment weight is approximately 50 kg including the TLS, batteries, tripod, operation computer and 3D targets.

### 3.3. Data specifications and preparation

The detailed scanning of the forest structure was done using stepwise horizontal and vertical TLS. A tripod was used to position the instrument approximately 1.5 m above the ground. Scanning was done outside and inside the vegetation patches. Resulting distance to the trees varied according to parameters from Table 1; it was 5 to 15 m for secondary vegetation (Fig. 1, No. 3). Due to the high density of juvenile trees and herbaceous plants in succession patches, two of the scans were taken from a platform 2.3 m above the ground. On average  $8 \pm 2$  scans were done on each forest type. Different opening angles were used, ranging from 180 to 360 degrees of horizontal sweep (depending on the structure) and 70 degrees of vertical sweep; distance from the target ranged from 5 to 80 m, adjusting the resolution for all scans to 0.02 m. For this study we did not use a total station (to reduce extra weight), instead we used 12 low-cost 3D targets, hand-made with a retro-reflective surface and light materials (~10 cm diameter foam rubber spheres and 1-in. polyvinyl chloride tubes of 1.2 m length). 3D targets were set on different positions for each patch so that at least three equal targets scans were captured by the two following scans. After finishing the scans, a sub scan section was added for the 3D targets adjusting the resolution to 0.002 m.

Each scan was set on the highest possible angular resolution, resulting in point clouds of 70,000 to 170,000 points on forest stratum. The variation in point density was assumed to be the result of variation in range, wind, temperature, and humidity, on both, the target and on air. Every single patch has an independent 3D point cloud, and manual measurements of the trees enable a comparison of the accuracy of the TLS data. Each scan was aligned into the same global coordinate system using the alignment tool of Cloud Compare (CC-V2) called “align by spheres”, for all the cases the precision error was <1 cm.

The total scanned area was 4.2 ha, which resulted in a 3D point cloud with over 138.6 million points of the two forests, covering 3 different patches: pine forest (25%), mature cypress forest (unburned area) (41%) and cypress forest with 8-year succession (burned area) (33%).



Fig. 3. Example of the 3 forest canopy layers at one cypress forest site at Guadalupe Island, dashed line represents the fourth layer mentioned in literature reviewed.

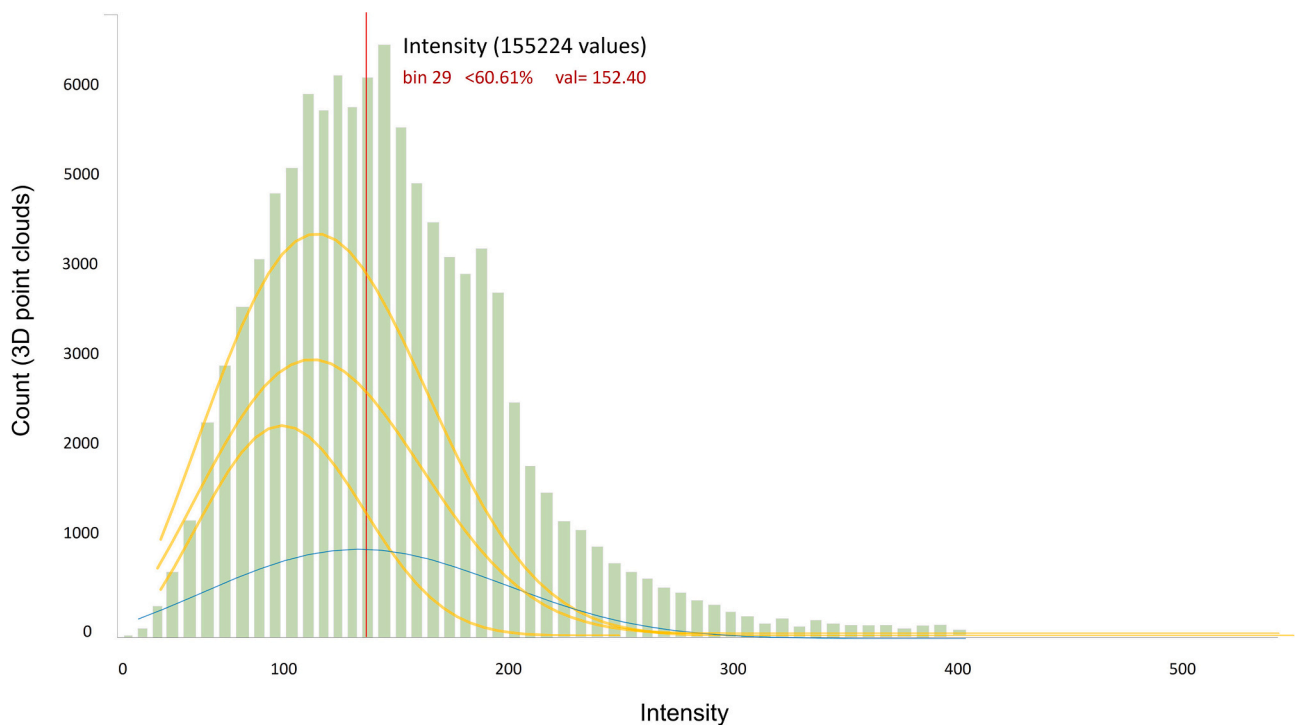


Fig. 4. Example of binned intensity histogram for the lower stratum (herbaceous understory) of the cypress forest in succession, Gaussian model in blue line and inverse Gaussian in yellow. (For interpretation of the references to colour in this figure legend, the reader is referred to the web version of this article.)

### 3.4. 3D-structural classification method (3D-SCM)

#### 3.4.1. Forest condition classification

3.4.1.1. *Height from surface.* We used the height from surface to segment the secondary succession forest complexity which is related to the forest canopy layers (Falkowski et al., 2009). Canopy height depends

on forest biodiversity and carbon cycling causing each plant species in the same forest succession to have a different height interval (Ma et al., 2015). The strata can be divided into imaginary horizons (Fig. 3) in the field, but with 3D information from TLS data, they can be extracted (de Moura et al., 2020). Canopy layers or height thresholds were determined based on literature about forests in succession, then forest strata were divided in four sections (Campbell et al., 2018; Nudds, 1977): (1) the

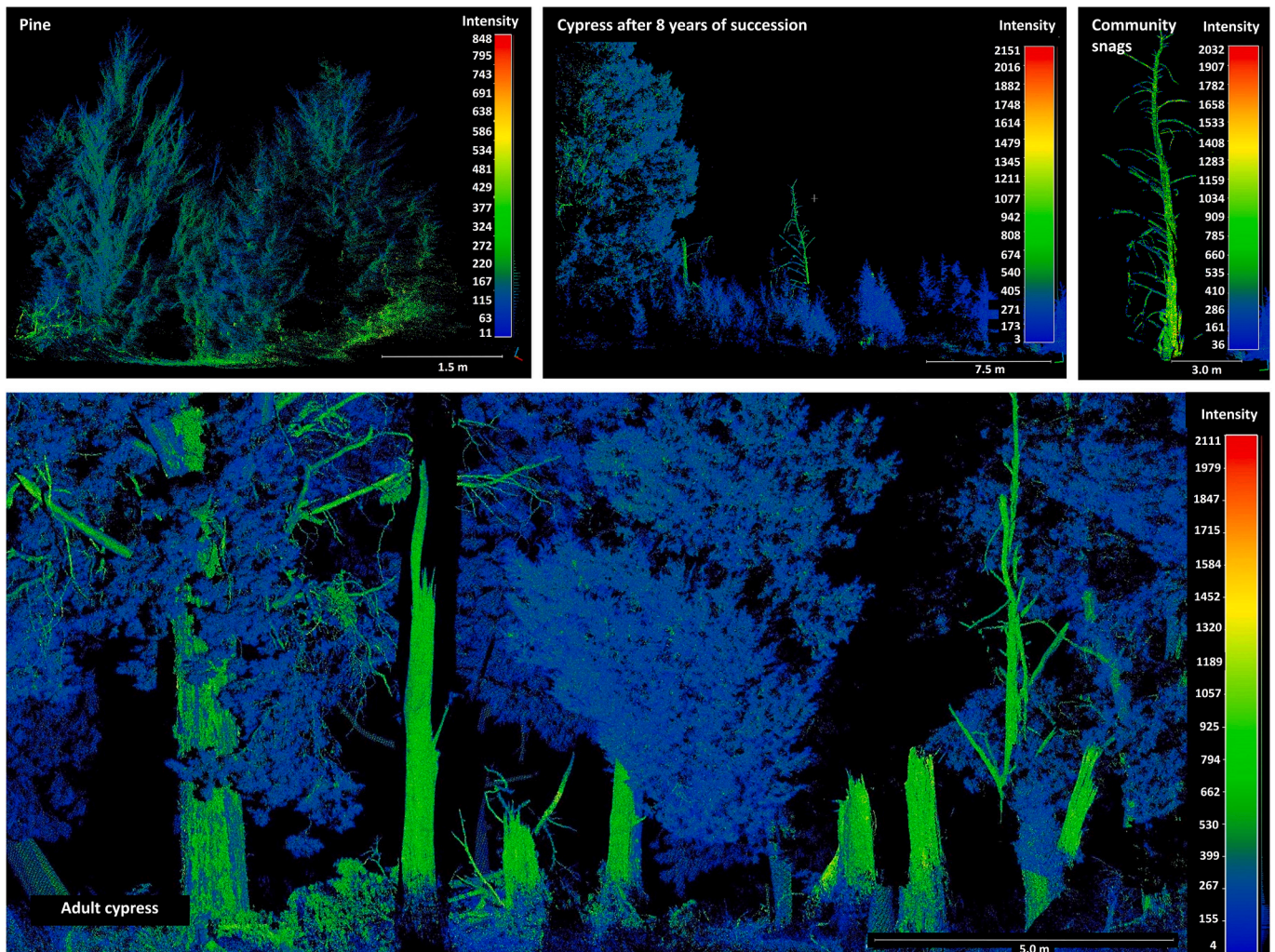


Fig. 5. Intensity ranges of adult cypress trees and juvenile pines. Values differ for foliage, snags, dead branches on trees, and herbaceous understory vegetation.

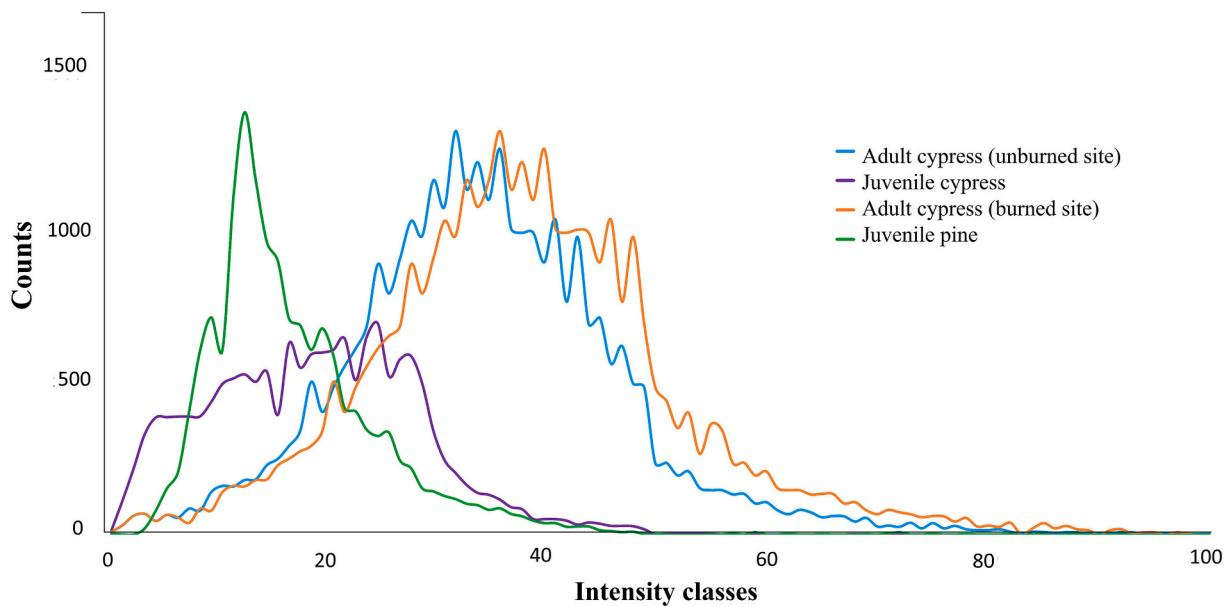
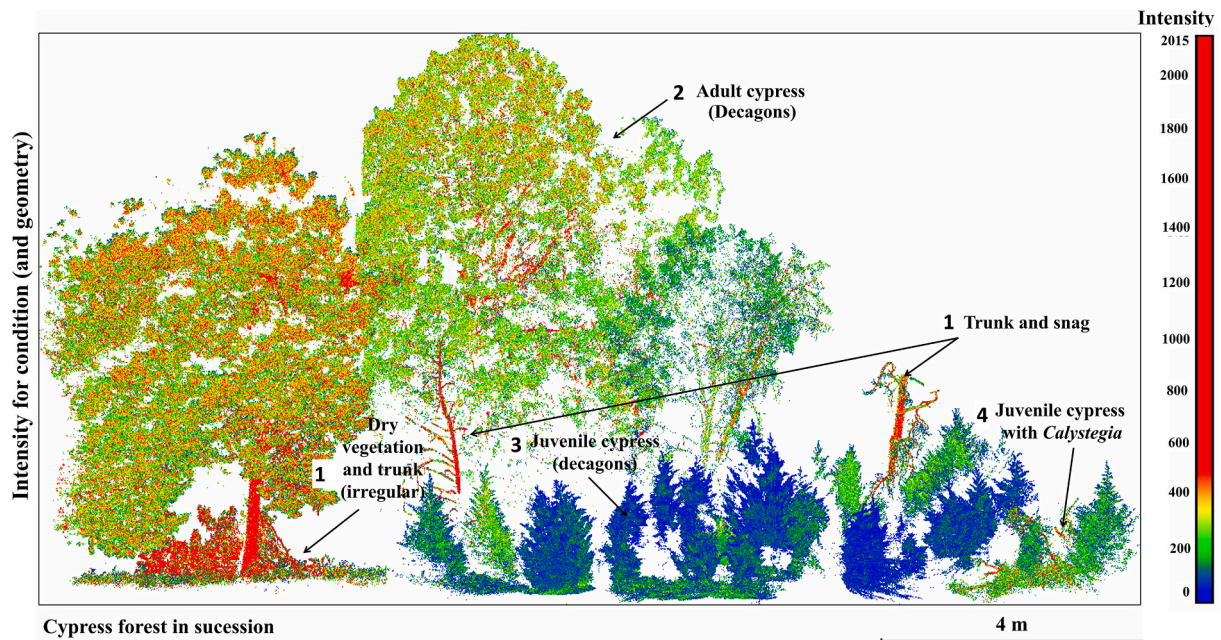


Fig. 6. Relative frequency distribution envelopes of intensities in binned classes of four types of canopy and disturbance factor for Guadalupe cypress and pines.



1. Dry herbaceous vegetation (*Calystegia*), cypress trunk and snags (herbaceous and woody understorey) / highest intensity values / irregular shape
2. Adult cypress ( overstorey) / middle intensity values / decagons or irregular shape
3. Juvenile cypress (herbaceous and woody understorey) / lowest intensity values / decagon shape
4. Juvenile cypress with *Calystegia* (herbaceous understorey) / middle intensity values /irregular shape

Fig. 7. Front section 3D point cloud of the Guadalupe cypress forest with intensities indicating different elements. The figure details canopy layer, intensity value rank and characteristic shape per element.

Table 2

Results of the probability density functions to estimate intensity ranges on the different forest community and disturbance factor, SD is the Standard Deviation and NA is not applicable.

Layers	Intensity Statistics	Pine-juvenile	Cypress-adult	Cypress-snags (burned)	Cypress-juvenile
Canopy	Mean	30.6	312.91	194.21	55.13
	SD	11.53	40.11	25.7	11.42
	IGaussian	$\lambda = 1.2675 \mu = 30.6$	$\lambda = 112.04 \mu = 312.91$	$\lambda = 7.29 \mu = 262.02$	$\lambda = 7.55 \mu = 55.13$
	Raleigh	NA	$\sigma = 249.67$	$\sigma = 317.44$	NA
	Wiebull	$\alpha = 0.41 \beta = 20.09$	NA	NA	NA
	Chi-Squared	NA	NA	NA	$\nu = 2$
	Forest Srata	2 to 25 m	6 to 28 m	6 to 26 m	0.15 to 3 m
Trunk, snags and branches	Mean	40.85	75.58	194.21	8.82
	SD	6.29	9.49	25.7	2.88
	IGaussian	$\lambda = 40.504 \mu = 262.91$	$\lambda = 6.036 \mu = 109.82$	$\lambda = 3.77 \mu = 31.61$	$\lambda = 0.49 \mu = 8.82$
	Raleigh	NA	$\sigma = 60.31$	NA	NA
	Wiebull	NA	NA	NA	$\alpha = 0.56 \beta = 10.0$
	Chi-Squared	$\nu = 2$	NA	$\nu = 2$	NA
	Forest Srata	1.5 to 25 m	1.5 to 10 m	1 to 25 m	0 to 2 m
Ground and/or grasses	Mean	75.81	95.83	262.91	152.1
	SD	13.89	11.1	51.37	26.09
	IGaussian	$\lambda = 1.2675 \mu = 30.6$	$\lambda = 5.24 \mu = 127.27$	$\lambda = 40.50 \mu = 262.91$	$\lambda = 30.59 \mu = 152.4$
	Raleigh	NA	$\sigma = 141.17$	NA	NA
	Wiebull	$\alpha = 0.41 \beta = 20.09$	NA	NA	NA
	Chi-Squared	NA	NA	$\nu = 2$	$\nu = 2$
	Forest Srata	0 to 1.5 m	0 to 1.5 m	0 to 1 m	0 to 2.5 m

herbaceous understorey that includes grasses, shrubs and juvenile trees (seedlings and saplings) (0 to <1.5 m); (2) the woody understorey, that includes adult tree trunk and branches of adults (1.5 to 8 m); (3) the midstorey, i.e. trees below the overstorey and above the understorey and (4) the overstorey or canopy of the forests ( $\geq 8$  m), the most dense part of the vegetation.

3.4.1.2. Intensity data classification. The intensity data classification was done on two scenarios: (1) the pine forest and the unburned cypress forest with adults and snags, and (2) the burned cypress forest (from the

2008 fire) which is a successional area with juvenile trees and secondary vegetation. Intensity measurements were processed directly with no corrections since the measurement distance (5 to 80 m) was not significant to consider distortions. Using intensity and geometric data classification, through CANUPO, a plugin available in CC-V2, the point clouds were segmented automatically into foliage, woody parts and snags (including burned trees). A dense point cloud with intensity values from the TLS allows mapping these complex scenarios. Fig. 4 shows an intensity profile at the cypress central site with adult trees and snags.

From the TLS sampled data, individual tree point clouds were

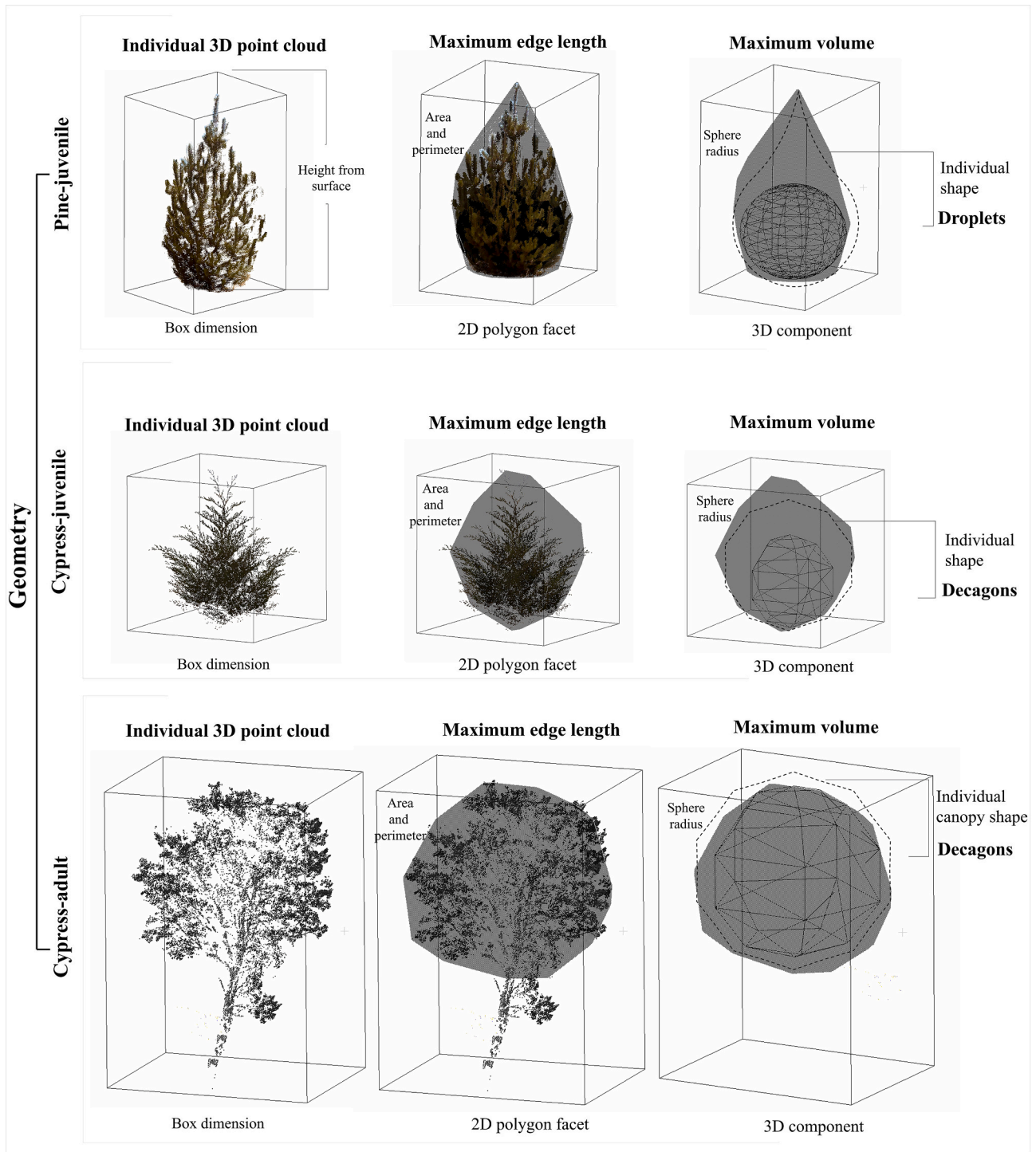


**Fig. 8.** Individual shape analysis using geometry of 2D polygon facet and spherical radius based on a 3D point cloud. The best fit was a Droplet for juvenile pine (A), and Decagons for adult and juvenile cypress (B)(C).

manually selected (around  $3 \pm 1$  per forest canopy layer) and 4 samples for each part of the tree were analyzed (leaves, branches, and trunk) to determine their intensity ranges and frequency distribution. Probability density functions have been used systematically in remote sensing research to understand the radiative transfer behavior of objects (Cheng, 1995; Comaniciu and Meer, 2002; Dai et al., 2019). Intensity ranges of the selected point clouds were analyzed using four probability density functions: Inverse Gaussian, Rayleigh, Weibull, and Chi-Square models (Eqs. 1 to 4).

Inverse Gaussian distribution

$$f(x) = \sqrt{\frac{\lambda}{2\pi x^3}} \exp\left(-\frac{\lambda(x-\mu)^2}{2\mu^2 x}\right) \quad (1)$$

where  $\lambda$  is a continuous parameter ( $\lambda > 0$ ) and  $\mu$  is a continuous parameter ( $\mu > 0$ ).

Raleigh distribution

$$f(x) = \frac{x-\gamma}{\sigma^2} \exp\left(-\frac{1}{2}\left(\frac{x-\gamma}{\sigma}\right)^2\right) \quad (2)$$

**Table 3**  
 Statistics for the 2D and 3D geometrical concept. ¥ Variables used to estimate the Individual Shape Index.

Height range (m)	Individual Point cloud (x 1000)		2D Polygon Facet		Sphere Radius (m) ¥	Height Average (m) ¥	rSR¥	rSH¥	ISI¥
			Surface (m2) ¥	RMS					
Guadalupe Pine									
≤1.5	Mean	30.95	10.72	0.37	1.35	1.41	0.41	0.53	0.77
	SD	34.65	5.50	0.15	0.14	0.18			
1.5–8	Mean	100.20	35.35	0.59	2.36	5.32	0.84	0.95	0.89
	SD	147.78	6.72	0.22	0.19	0.68			
≥8.1	Mean	209.32	60.38	0.74	3.08	8.54	0.88	0.88	1.00
	SD	284.48	7.52	0.19	0.23	0.89			
Guadalupe Cypress									
≤1.5	Mean	0.40	0.90	0.14	0.39	1.31	0.83	0.69	1.20
	SD	0.34	0.61	0.07	0.08	0.25			
1.5–8	Mean	6.967	4.28	0.23	0.84	3.51	0.61	0.54	1.10
	SD	0.05	3.41	0.09	0.29	1.05			
≥8.1	Mean	444.26	60.83	0.80	3.94	11.42	0.45	0.34	1.35
	SD	79.71	15.67	0.27	0.51	2.19			

where  $\sigma$  is a continuous scale parameter ( $\sigma > 0$ ), and  $\gamma$  is a continuous location parameter ( $\gamma = 0$  yields the one parameter on Raleigh distribution).

Weibull distribution

$$f(x) = \frac{\alpha}{\beta} \left(\frac{x}{\beta}\right)^{\alpha-1} \exp\left(-\left(\frac{x}{\beta}\right)^\alpha\right) \quad (3)$$

where  $\alpha$  is the continuous shape parameter ( $\alpha > 0$ ), and  $\beta$  is the continuous parameter ( $\beta > 0$ ).

Chi-squared distribution

$$f(x) = \frac{(x-\gamma)^{\nu/2-1} \exp(-(x-\gamma)/2)}{2^{\nu/2} \Gamma(\nu/2)} \quad (4)$$

where  $\nu$  is the degrees of freedom (positive integer),  $\gamma$  is the continuous location parameter ( $\gamma = 0$  yields the one-parameter Chi-squared distribution) and  $\Gamma$  is the Gamma Function.

Intensity ranges were selected from the statistical values obtained from the Inverse Gaussian model, which is shown on Fig. 5 with an example of the Guadalupe cypress responses. This model represented an accurate display of the tree reflectivity.

### 3.4.2. Individual shape index (ISI)

**3.4.2.1. Intensity and geometry.** To recognize the geometrical features that characterize point clouds we used CANUPO (Brodu and Lague, 2012). This software distinguishes the heterogeneity of natural surfaces and their distinctive properties, allowing the automatic segmentation of point clouds, offering the possibility to split individuals or even parts of the tree. It has been applied for TLS data on forest ecology studies (Danson et al., 2018), and proven to be effective compared to other point cloud classification methods (Li et al., 2019). This tool allowed us to see horizontally separate individuals and to obtain individual segmentation and height from the data collected.

**3.4.2.2. Geometry.** A total of 140 individual trees were selected and exported as individual point clouds (70 for pine and 70 for cypress). We planned to analyze 70% of juvenile trees and 30% of adult trees, to be able to find the appropriate shape that fits each forest and to have the representative characteristics for the trees in each age class. Ninety-four of the selected trees were also inventoried using field techniques, measuring heights with a Suunto Pm-5 / 360 Pc Opti Clinometer and diameter breast height (DBH) using a TRUPER TP50ME Fiberglass Long Tape Rule. Height and crowns were taken from each individual tree and compared through a linear analysis based upon both techniques (TLS and field measurements).

The geometry analysis was performed individually (one per tree),

recording the location (XY) and tree height (Z). After this, we applied the Fit 2D Polygon facet and the Fit Sphere (CC-V2) analysis. The 2D polygon uses the maximum edge length out of 3 to 30 sections and then draws the best vertical plane into a 2D polygon, the output are the plane surface and the RMS (root mean square). The planes obtained were different for each species; for the cypress (both adult and juvenile) the best fit was a decagon shape (10 sides) and for the pine a droplet shape was selected. Additionally, the Fit Sphere creates the 3D component by automatically fitting a sphere primitive contained within each tree point cloud, simulating the canopy. From the geometry analysis we estimated three values for building the ISI: (1) height; (2) surface in square meters (sqm); and (3) sphere radius (m).

**3.4.2.3. Building the ISI.** Pine and cypress forests have unique shape characteristics. We used the Pearson's Correlation Coefficient (PCC) (Eq. (5)) to assess the linear relationship between the variables: 1) surface - height (SH); and 2) surface- radius (SR).

$$r = \frac{N\sum xy - (\sum x)(\sum y)}{\sqrt{[N\sum x^2 - (\sum x)^2][N\sum y^2 - (\sum y)^2]}} \quad (5)$$

where:

r = relation for each combination (SR or SH).

N = number of pair of scores.

$\sum xy$  = sum of the products of paired scores.

$\sum x$  = sum of x scores.

$\sum y$  = sum of y scores.

$\sum x^2$  = sum of squared x scores.

$\sum y^2$  = sum of squared y scores.

Then, we calculated the shape index.

$$ISI = \frac{rSR}{rSH} \quad (6)$$

where:

rSR = linear correlation surface- radius.

rSH = linear correlation surface-height.

## 4. Results

### 4.1. Forest condition classification

Height from surface.

The height of the general point cloud ranged from 0.29 m to 38.6 m. The forest strata have interval heights of 2 to 25 m for the canopy of the primary vegetation and 0 to 1.5 m for the ground, grasses, and secondary vegetation. The segmentations created with trunks, snags and

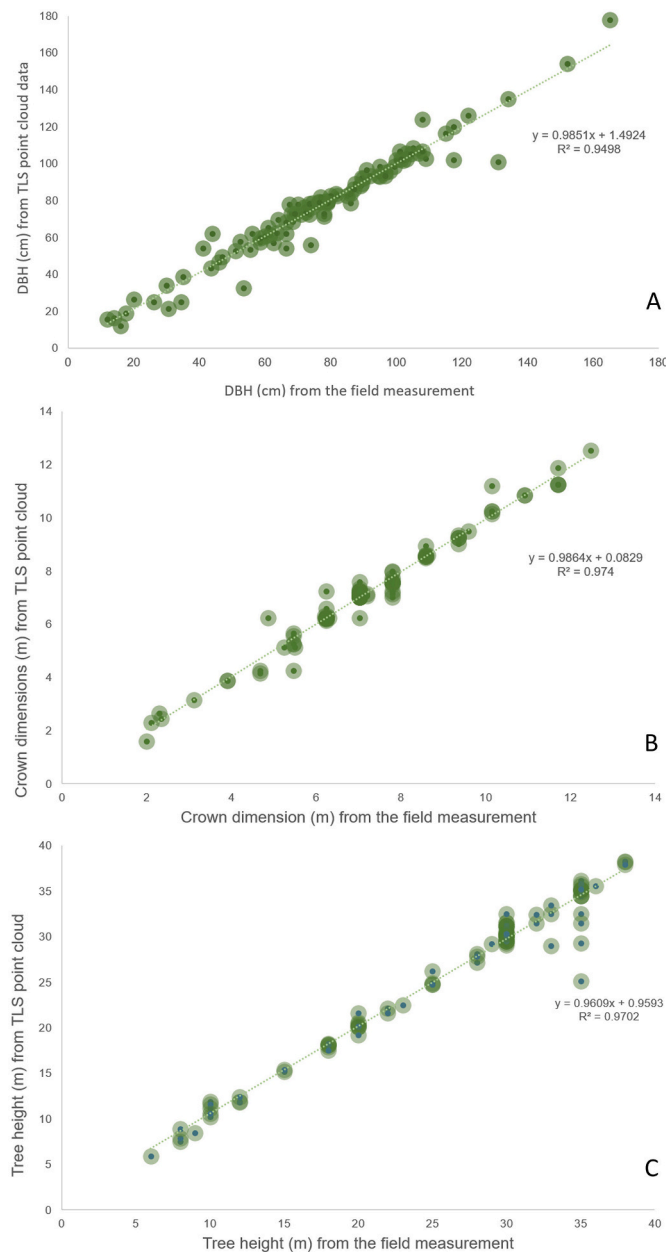


**Fig. 9.** Relationship between the A) diameter breast height, B) crown diameter and C) tree heights obtained with the TLS and the field inventoried sample.

branches were taken from 1.5 to 25 m.

**Intensity data classification.**

The range of intensity for samples of the adult pine forest was 11 to 848 (Fig. 5), and 7 to 1392 for the canopy of the juvenile pine forest. Intensity values for The Guadalupe cypress forest ranged from 3 to 2151 (Fig. 5), and from 2 to 712 for the canopy of juvenile cypress. Snags (burned trees) had intensities that ranged from 36 to 2032 (Fig. 5). The canopy intensities for adult cypress on the burned site ranged from 3 to 692. The relative intensity frequency distributions of four of the classes analyzed are presented in Fig. 6. A difference between juvenile and adult individuals can be perceived, with lower intensities on the juveniles. Also, a distinction between burned and unburned adults was apparant, with slightly higher intensities on the burned ones.

The intensity values and the geometrical characteristics are presented in Fig. 7. Applying the intensity filters allowed us to map the 3D structure profiles, identifying different elements of the forests, even at the most complex images (the ones that contained a mix of elements as

snags, juvenile trees, dry shrubs, forbs, etc.; Fig. 7). The results of intensity filters can be seen in Table 2, the best segmentation was made with the inverse Gaussian function after 3 run models, resulting in 75%, 83% and finally 91% of precision.

Adult trees were located in all sampled forests. Juvenile trees were in the Guadalupe cypress forest, especially in the burned area. The cypress forest in succession was the most complex forest; intensity values were diverse due to the presence of juvenile cypress, the Calystegia foliage or snags.

**4.2. Individual shape index (ISI)**

ISI demonstrates that pine and cypress have a distinctive shape (Fig. 8). The best shape fit for the juvenile pine was a Droplet (Fig. 8A) and decagons best fit for cypress, both adult and juvenile individuals (Fig. 8B and C; Table 3). Using the ISI, we identified 24 adults (height between 10 and 32 m); 59 juveniles (height between 3 and 10 m); and 82 reborns (height between 0.1 and 3 m). For the pine forest, we identified 38 juvenile pines with height ranging from 1.5 to 12 m.

The sphere radius value ranged from 0.14 m to 3.08 m for pines; and 0.39 m to 3.94 m for cypress (Table 3), but generally increased with each canopy layer. Surface and sphere radius values were used to estimate the ISI. When ISI values near 1.0 the shape of the tree is geometrically balanced, this was observed for adult Guadalupe pines  $\geq 8.1$  m and for Guadalupe cypress from 1.5 to 8 m.

Geometry was validated using field measurements and a linear relation of height and crown diameter for the inventoried tree sample. Results in Fig. 9 indicate a strong linear correlation between the geometry dimensions taken with TLS and the traditional measurements in field  $R^2 = 0.949$  for DBH,  $R^2 = 0.974$  for the crown and  $R^2 = 0.97$  for heights.

**4.3. 3D-SCM**

The classification of the 3D point clouds resulted from the segmentation of distinctive classes along the vegetation structure. The classification used filtering method that clusters the intensity, similar to other studies using ALS or TLS (Singh et al., 2020; Zhu et al., 2018), which consider intensity values, tree height and geometrical characteristics of the elements to segment the point cloud into classes. The 3D-SCM had different outputs such as: a) the individual trees height estimate (Fig. 10A); b) the segmentation by classes of woody or non-woody elements such as the leaves and trunks (Fig. 10B); c) the greenness of vegetation recorded as intensities (Fig. 10C and D); d) the different conditions showing age class (adult or juvenile) cypress (Fig. 10E); and e) the condition e.g. burned trees (Fig. 10F). The efficiency of the method was evaluated at the stand level using the classes of adult cypress, juvenile cypress, adult cypress burned and juvenile pine retrieving an accuracy of the 93%, while for the tree level classification composed by leaves, branches, trunks and snags reached 97% (Table 4).

**5. Discussion**

Through this research we strived to characterize physical and spatial properties of the species from an endemic forest in a critical situation. The integration of the FCC achieves the representation of forest canopy layers with vertical characteristics of height and intensity values, while the ISI generates specific metrics and shape of the individual trees. The 3D structural classification profile was possible with the implementation of 3D-SCM using TLS. TLS was crucial for this study considering that on airborne scanner studies has below 50% detection of the under-story individual trees (Hamraz et al., 2017). 3D-SCM maps canopy layers and tree vertical structure (stem, branches, and leaves) which helps to quantify the success of forest management practices.

The adult result tree heights have a high correlation with previous field studies, that were made in 1996 and 2006, with 12–20 m for adult

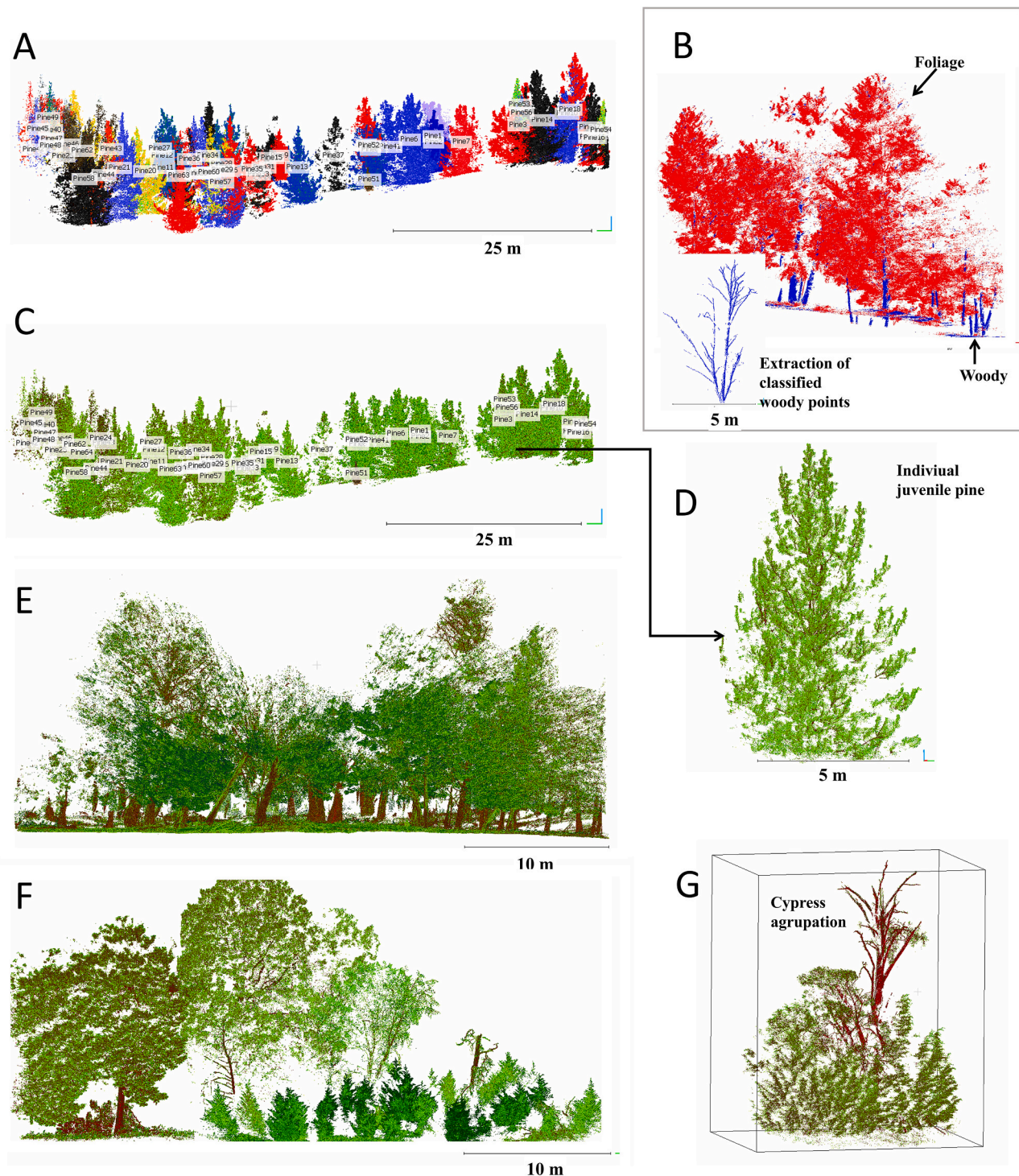


**Fig. 10.** Results of the classification of the frontal view of the vertical structure of (A)(C) pine forest, individual point clouds, (B) mature cypress forest foliage in red, and woody points in blue; (E) mature cypress forest, unburned site; (F) cypress forest, adults, juveniles, and snags (burned trees); (G) dense vegetation in succession in cypress forest: dead trees, juveniles, Calystegia. (For interpretation of the references to colour in this figure legend, the reader is referred to the web version of this article.)

cypress and less than 30 for pine (Oberbauer et al., 2009; Garcillán et al., 2009; Moran, 1999) three years after goat eradication on Guadalupe Island, Moran, 1999). The limited access to the island made difficult to perform an exhaustive field work, previous studies were made with qualitative methods. This kind of work will contribute to a precise quantitative research of the forest statistics in remote places with restricted access.

### 5.1. FCC

The use of probability density functions to detect intensity ranges was crucial to find the intervals among each class variation. The combination of elements (plant species) caused a mix of classes of 3D point, this complexity increased for the data where species overlapped which affected their reflection. The symbiotic relationship between Calystegia, a vine which covers the tree, and juvenile cypress is an example of this

**Table 4**  
Error matrix classification tree algorithm for A) Stand level profile and B) Tree level profile.

A	Manual classified points	Automatic classified points				
		Adult cypress	Juvenile cypress	Adult cypress burned	Juvenile pine	Total reference points
Stand level	Adult cypress	209,657	1442	842	912	212,853
	Juvenile cypress	1254	53,978	1254	5468	61,954
	Adult cypress burned	1065	123	16,154	852	18,194
	Juvenile pine	1245	6985	1511	26,524	36,265
	Total classified points	213,221	62,528	19,761	33,756	329,266
	Manual classified points	Automatic classified points				
B		Leaves	Branches	Trunk	Snags	Total reference points
	Tree level	Leaves	Branches	Trunk	Snags	Total reference points
	Leaves	352,622	562	1554	2653	357,391
	Branches	2468	23,512	325	445	26,750
	Trunk	1205	1264	48,263	2561	53,293
	Snags	1268	148	1544	26,520	29,480
	Total classified points	357,563	25,486	51,686	32,179	466,914
Stand level classification		Total points			User's accuracy	Producer's accuracy
Total correct reference points		306,313	A	Adult cypress	98.5	98.33
Total true reference points		329,266		Juvenile cypress	87.13	86.33
Percent accuracy		0.93		Adult cypress burned	88.79	81.75
					78.58	89.81
Tree level classification		Total points	B	Leaves	98.67	98.62
Total correct reference points		450,917		Branches	87.9	92.25
Total true reference points		466,914		Trunk	90.56	93.38
Percent accuracy		0.97		Snags	89.96	82.41

overlap, complicating the discrimination of classes between the two species. However, this method achieves in a third run a 91% precision with the function's combination, a little bit more than using only the Gaussian method (87.68%, Hui et al., 2021).

The collection of point clouds extracted using their intensity values and height was useful to identify the forest condition and canopy layers. Each forest had a unique spectral characteristic as well as each component of the tree. This finding permitted the classification by individual structural part; however, it was only possible with individuals where the laser beam was able to penetrate to the trunk. Using satellital images it is possible to map the canopy diameter but is almost impossible to collect data of trunks, areal laser scanning has the potential of collect some trunks, but get branches and leaves is a unique advantage of TLS scanners. Although, it is important to point out that the TLS used has only 1 return per register. It does not have typical problems of satellite images as problems of double-sided illumination, shadow, and mixed pixels and aerial scanning like loss of recognition by canopy strata (Hamraz et al., 2017). As expected, canopy leaves reported the smallest intensity values. This is because intensity is the value of reflectivity, which is a function of the surface texture, roughness, and the interaction with the near infrared wavelength of the laser pulse, modulating the amount of energy reflected back to the sensor. On the contrary than other referenced researches (Singh et al., 2020), in this study distance measurements were not considered to cause a significant distortion of the results. This assumption is due GLS 1500 laser sensor works in an optimal range of 150 m, as long as when the rebound is from a dry surface with normal reflectivity (Bråtveit et al., 2012), besides sunlight conditions during research period were similar among scans, which means that the noise was minimum (Pomerleau et al., 2012).

### 5.2. Individual shape index

Guadalupe cypress and Monterrey pine individuals present in the Guadalupe Island have very distinctive geometrical characteristics in the adult form. The ISI based function allows to measure and quantify this difference. The shapes described in the ISI for the mature pines and cypress are commonplace for other locations, specifically neotropical pines that may encounter frequent fire, self-prune, or at old growth stature become flat-top. This is not the case for juveniles due to the similarity in shape of both species at this age. Geometrical balance is displayed for adults of Guadalupe pines and for juveniles of Guadalupe cypress. Succession zones are complex to map due to the diversity of

shapes and sizes of the species present in burned areas. Similar algorithms are used to recognize different species in large datasets (Ferraz et al., 2016) and that was possible to test in the study site, although the total extent of the scanned area only represents the 6.4% of the forest coverage on the island, we believe that the results are representative for both forests.

### 5.3. 3D-SCM

FCC or ISI can be used independently, however, the synergy of both processes allows the complete development of 3D-SCM. The advantage of implementing 3D-SCM is that the uncertainty about class determination is reduced in the different conditions present on the island, such as burned and unburned areas, different types of forests, and different species or ages.

The use of 3D-SCM also permits non-invasive precise estimations of the tree biomass, which is key for endangered species such those in the forest of Guadalupe Island. To date, as part of a restoration project implemented on site since 2014, more than 100,000 plants have been reforested to restore the forest original coverage (Garcillán et al., 2009). These actions will improve the forests and habitat for native fauna and the environmental services. Carbon sequestration is one of these services because forests act as carbon sinks. The typical way to estimate the forest biomass is to calculate the individual tree biomass using allometric equations and information of the stem diameter at DBH and tree height (H) (Change, 2007; Návar, 2009). The alternative is the use of tree-lethal (destructive methods) to quantify the dry weight of each component (Nogueira et al., 2008), which is not always feasible. 3D-SCM is a LIDAR segmentation process that outperforms the traditional methods. The specific gadget (GLS 1500) that was used for this study limited the mobility due to the weight, however new lighter instruments are emerging. This would benefit the research done for remote areas like Guadalupe Island.

## 6. Conclusions

Before 2016, forest assessments in Guadalupe Island were based on qualitative measurements or 2D coverage estimates. In this study, a novel methodology based on Terrestrial Laser Scanner was implemented through the 3D Structural Classification Method (3D-SCM). The main contribution of 3D-SCM is mapping canopy layers, individual trees, and even architectural tree level classes. In addition, geometrical

information throughout the Individual Shape Index is achieved by determining the best characteristic shape for the Guadalupe cypress (decagon) and for the pine (droplet) which is an innovative way to rapidly determine species and age. Results demonstrate that 3D-SCM is an accurate digital tool for updating forest inventories in the Guadalupe Island. It would be possible to implement the 3D-SCM in other islands or forests with similar characteristics, but prior calibration is needed.

The synergy of the 2D and 3D remote sensors collected digital data for a complete spatial and physical characterization of the forest recovery process in Guadalupe Island. This process can be replicated for monitoring patches or tree individual trees to predict successional trends. This 3D vertical structure assessment enhances and improves accuracy of measurements to better understand succession of the Guadalupe Island ecosystem.

## Funding

This research was funded by GECEI (Grupo de Ecología y Conservación de Islas, A.C.), Comisión Nacional Forestal, Universidad Autónoma de Nuevo León and Mexican Secretariat of Public Education (SEP-PRODEP).

## Declaration of Competing Interest

The authors declare no conflict of interest.

## Acknowledgments

We thank all biologist and personal from GECEI and the Centro de Investigación Científica y de Educación Superior de Ensenada Baja California (CICESE), and thanks to William D. Eldridge for his support and comments.

## References

- Aguirre-Muñoz, A., Samaniego-Herrera, A., Luna-Mendoza, L., Ortiz-Alcaraz, A., Rodríguez-Malagón, M., Méndez-Sánchez, F., Félix-Lizárraga, M., Hernández-Montoya, J.C., González-Gómez, R., Torres-García, F., 2011. Island Restoration in Mexico: Ecological Outcomes after Systematic Eradications of Invasive Mammals. *Island Invasives. Eradication and Management*, pp. 250–258.
- Aldred, A.H., Bonnor, G.M., 1985. Application of airborne lasers to forest surveys, vol. 51.
- Bergen, K.M., Gilboy, A.M., Brown, D.G., 2007. Multi-dimensional vegetation structure in modeling avian habitat. *Ecological Informatics* 2 (1), 9–22.
- Bournez, E., Landes, T., Saudreau, M., Kastendeuch, P., Najjar, G., 2017. March. From TLS point clouds to 3D models of trees: a comparison of existing algorithms for 3D tree reconstruction. In: 3d virtual reconstruction and visualization of complex architectures, vol. 42. Copernicus Gesellschaft MbH, pp. 113–120 no. 2.
- Bråtevit, K., Lia, L., Olsen, N.R.B., 2012. An efficient method to describe the geometry and the roughness of an existing unlined hydro power tunnel. *Energy Procedia* 20, 200–206.
- Brodu, N., Lague, D., 2012. 3D terrestrial lidar data classification of complex natural scenes using a multi-scale dimensionality criterion: applications in geomorphology. *ISPRS J. Photogramm. Remote Sens.* 68, 121–134.
- Calders, K., Armston, J., Newnham, G., Herold, M., Goodwin, N., 2014. Implications of sensor configuration and topography on vertical plant profiles derived from terrestrial LiDAR. *Agric. For. Meteorol.* 194, 104–117.
- Calders, K., Newnham, G., Burt, A., Murphy, S., Raunonen, P., Herold, M., Culvenor, D., Avitabile, V., Disney, M., Armston, J., 2015. Nondestructive estimates of above-ground biomass using terrestrial laser scanning. *Methods Ecol. Evol.* 6 (2), 198–208.
- Campbell, M.J., Dennison, P.E., Hudak, A.T., Parham, L.M., Butler, B.W., 2018. Quantifying understory vegetation density using small-footprint airborne lidar. *Remote Sens. Environ.* 215, 330–342.
- Change, C., 2007. Synthesis Report. Contribution of Working Groups I, II and III to the Fourth Assessment Report of the Intergovernmental Panel on Climate Change. IPCC, Geneva, Switzerland.
- Cheng, Y., 1995. Mean shift, mode seeking, and clustering. *IEEE Trans. Pattern Anal. Mach. Intell.* 17 (8), 790–799.
- Comaniciu, D., Meer, P., 2002. Mean shift: a robust approach toward feature space analysis. *IEEE Trans. Pattern Anal. Mach. Intell.* 24 (5), 603–619.
- CONANP, 2013. Programa de Manejo Reserva de la Biosfera Isla Guadalupe. Comisión Nacional de Áreas Naturales Protegidas.
- Cramer, W., Bondeau, A., Woodward, F.I., Prentice, I.C., Betts, R.A., Brovkin, V., Cox, P. M., Fisher, V., Foley, J.A., Friend, A.D., 2001. Global response of terrestrial ecosystem structure and function to CO<sub>2</sub> and climate change: results from six dynamic global vegetation models. *Glob. Chang. Biol.* 7 (4), 357–373.
- Cruz, L., Lucio, D., Velho, L., 2012. Kinect and RGBD images: challenges and applications. In: *Proceedings: 25th SIBGRAPI - Conference on Graphics, Patterns and Images Tutorials, SIBGRAPI-T 2012, August*, 36–49. <https://doi.org/10.1109/SIBGRAPI-T.2012.13>.
- Dai, W., Yang, B., Liang, X., Dong, Z., Huang, R., Wang, Y., Li, W., 2019. Automated fusion of forest airborne and terrestrial point clouds through canopy density analysis. *ISPRS J. Photogramm. Remote Sens.* 156, 94–107.
- Ferraz, A., Saatchi, S., Mallet, C., Meyer, V., 2016. Lidar detection of individual tree size in tropical forests. *Remote Sens. Environ.* 183, 318–333.
- Danson, F.M., Sasse, F., Schofield, L.A., 2018. Spectral and spatial information from a novel dual-wavelength full-waveform terrestrial laser scanner for forest ecology. *Interface Focus* 8, 20170049.
- de Gouvenain, R.C., Ansary, A.M., 2006. Association between fire return interval and population dynamics in four California populations of Tecate cypress (*Cupressus forbesii*). *Southwest. Nat.* 51 (4), 447–454.
- de Moura, Y.M., Balzter, H., Galvão, L.S., Dalagnol, R., Espírito-Santo, F., Santos, E.G., Garcia, M., Bispo, P. da C., Oliveira, R. C., & Shimabukuro, Y. E., 2020. Carbon dynamics in a human-modified tropical Forest: a case study using multi-temporal LiDAR data. *Remote Sens.* 12 (3), 430.
- Disney, M., Burt, A., Calders, K., Schaaf, C., Stovall, A., 2019. Innovations in ground and airborne technologies as reference and for training and validation: terrestrial laser scanning (TLS). *Surv. Geophys.* 40 (4), 937–958.
- Estornell, J., Ruiz, L.A., Velázquez-Martí, B., Hermosilla, T., 2012. Estimation of biomass and volume of shrub vegetation using LiDAR and spectral data in a Mediterranean environment. *Biomass Bioenergy* 46, 710–721.
- Falkowski, M.J., Evans, J.S., Martinuzzi, S., Gessler, P.E., Hudak, A.T., 2009. Characterizing forest succession with lidar data: an evaluation for the inland northwest, USA. *Remote Sens. Environ.* 113 (5), 946–956.
- Fernandes, P.M., 2009. Combining forest structure data and fuel modelling to classify fire hazard in Portugal. *Ann. For. Sci.* 66 (4), 1–9.
- Franceschi, F., 1893. Notes on the flora of Guadalupe Island. *Zoe (1890–1906)*, 4(2), p. 130.
- García-Gutiérrez, C., Hinojosa-Corona, A., Franco-Vizcaíno, E., Riggan, P.J., Bocco, G., Luna-Mendoza, L., 2005. Cartografía base para la conservación de Isla Guadalupe. Avances, perspectivas y necesidades. In: *Isla Guadalupe, Restauración y Conservación*, pp. 19–25.
- Garcillán, P.P., Vega, E., López-Reyes, E., 2009. Recruitment response of Guadalupe cypress (*Callitropsis guadalupensis*) three years after goat eradication on Guadalupe Island. In: *Proceedings of the Seventh California Islands Symposium*, pp. 177–183.
- Goetz, S., Steinberg, D., Dubayah, R., Blair, B., 2007. Laser remote sensing of canopy habitat heterogeneity as a predictor of bird species richness in an eastern temperate forest, USA. *Remote Sens. Environ.* 108 (3), 254–263.
- Gower, S.T., Kucharik, C.J., Norman, J.M., 1999. Direct and indirect estimation of leaf area index, FAPAR, and net primary production of terrestrial ecosystems. *Remote Sens. Environ.* 70 (1), 29–51.
- Greene, E.L., 1885. Studies in the Botany of California and Parts Adjacent: I-VI. The Academy.
- Guo, Z., Feng, C.-C., 2020. Using multi-scale and hierarchical deep convolutional features for 3D semantic classification of TLS point clouds. *Int. J. Geogr. Inf. Sci.* 34 (4), 661–680.
- Hackenberg, J., Spiecker, H., Calders, K., Disney, M., Raunonen, P., 2015. SimpleTree—an efficient open source tool to build tree models from TLS clouds. *Forests* 6 (11), 4245–4294.
- Hamraz, H., Contreras, M.A., Zhang, J., 2017. Vertical stratification of forest canopy for segmentation of understory trees within small-footprint airborne LiDAR point clouds. *ISPRS Journal of Photogrammetry and Remote Sensing* 130, 385–392.
- Hansen, A.J., Rotella, J.J., 2000. Bird Responses to Forest Fragmentation. *Forest Fragmentation in the Southern Rockies*. University Press of Colorado, Boulder, pp. 201–219.
- Hopkinson, C., Chasmer, L., Young-Pow, C., Treitz, P., 2004. Assessing forest metrics with a ground-based scanning lidar. *Can. J. For. Res.* 34 (3), 573–583.
- Hui, Z., Jin, S., Li, D., Ziggah, Y.Y., Liu, B., 2021. Individual Tree Extraction from Terrestrial LiDAR Point Clouds Based on Transfer Learning and Gaussian Mixture Model Separation. *Remote Sensing* 13 (2), 223.
- Hyde, P., Dubayah, R., Walker, W., Blair, J.B., Hofton, M., Hunsaker, C., 2006. Mapping forest structure for wildlife habitat analysis using multi-sensor (LiDAR, SAR/InSAR, ETM+, Quickbird) synergy. *Remote Sens. Environ.* 102 (1–2), 63–73.
- Jehl, J.R., Everett, W.T., 1985. History and Status of the Avifauna of Isla Guadalupe, Mexico.
- Jung, S.-E., Kwak, D.-A., Park, T., Lee, W.-K., Yoo, S., 2011. Estimating crown variables of individual trees using airborne and terrestrial laser scanners. *Remote Sens.* 3 (11), 2346–2363.
- Kaasalainen, S., Krooks, A., Liski, J., Raunonen, P., Kaartinen, H., Kaasalainen, M., Puttonen, E., Anttila, K., Mäkipää, R., 2014. Change detection of tree biomass with terrestrial laser scanning and quantitative structure modelling. *Remote Sens.* 6 (5), 3906–3922.
- Kolecka, N., 2018. Height of successional vegetation indicates moment of agricultural land abandonment. *Remote Sens.* 10 (10), 1568.
- Kraus, K., Pfeifer, N., 1998. Determination of terrain models in wooded areas with airborne laser scanner data. *ISPRS J. Photogramm. Remote Sens.* 53 (4), 193–203.
- Lang, M.W., McCarty, G.W., 2009. Lidar intensity for improved detection of inundation below the forest canopy. *Wetlands* 29 (4), 1166–1178.

- Lefsky, M.A., Harding, D., Cohen, W.B., Parker, G., Shugart, H.H., 1999. Surface lidar remote sensing of basal area and biomass in deciduous forests of eastern Maryland, USA. *Remote Sens. Environ.* 67 (1), 83–98.
- Li, W., Guo, Q., Jakubowski, M.K., Kelly, M., 2012. A new method for segmenting individual trees from the lidar point cloud. *Photogramm. Eng. Remote Sens.* 78 (1), 75–84.
- Li, H., Meng, W., Liu, X., Xiang, S., Zhang, X., 2019. Parameter optimization criteria guided 3D point cloud classification. *Multimed. Tools Appl.* 78 (4), 5081–5104.
- Liang, X., Hyyppä, J., Kaartinen, H., Holopainen, M., Melkas, T., 2012. Detecting changes in forest structure over time with bi-temporal terrestrial laser scanning data. *ISPRS International Journal of Geo-Information* 1 (3), 242–255.
- Luna-Mendoza, L., Aguirre-Muñoz, A., Hernández-Montoya, J.C., Torres-Aguilar, M., García-Carreón, J.S., Puebla-Hernández, O., Luvianos-Colín, S., Cárdenas-Tapia, A., Méndez-Sánchez, F., 2019. Ten years after feral goat eradication: the active restoration of plant communities on Guadalupe Island, Mexico. In: *Island Invasives: Scaling up to Meet the Challenge*, 62, p. 571.
- Ma, L., Zheng, G., Eitel, J.U.H., Moskal, L.M., He, W., Huang, H., 2015. Improved salient feature-based approach for automatically separating photosynthetic and nonphotosynthetic components within terrestrial lidar point cloud data of forest canopies. *IEEE Trans. Geosci. Remote Sens.* 54 (2), 679–696.
- Maas, H., Bienert, A., Scheller, S., Keane, E., 2008. Automatic forest inventory parameter determination from terrestrial laser scanner data. *Int. J. Remote Sens.* 29 (5), 1579–1593.
- Macleay, G.A., Krabill, W.B., 1986. Gross-merchantable timber volume estimation using an airborne LIDAR system. *Can. J. Remote Sens.* 12 (1), 7–18.
- Magnusson, W.E., de Lima, O.P., Reis, F.Q., Higuchi, N., Ramos, J.F., 1999. Logging activity and tree regeneration in an Amazonian forest. *For. Ecol. Manag.* 113 (1), 67–74.
- McCaughy, R.J., Carson, W.W., Reutebuch, S.E., Andersen, H.-E., 2004. Direct Measurement of Individual Tree Characteristics from LIDAR Data. Proceedings of the Annual ASPRS Conference. American Society of Photogrammetry and Remote Sensing, Denver.
- Melling, A.E., 1985. Situación actual de la vegetación de Isla Guadalupe, BC, México, Tesis de licenciatura. Universidad Autónoma de Baja California, Ensenada.
- Moran, R., 1996. Flora of Guadalupe Island, Mexico. California Academy of Sciences.
- Moran, R., 1999. Guadalupe Island and its flora. *Fremontia*, special edition July 42–51.
- Moskal, L.M., Zheng, G., 2012. Retrieving forest inventory variables with terrestrial laser scanning (TLS) in urban heterogeneous forest. *Remote Sens.* 4 (1), 1–20.
- Návar, J., 2009. Allometric equations for tree species and carbon stocks for forests of northwestern Mexico. *For. Ecol. Manag.* 257 (2), 427–434.
- Nelson, R., Krabill, W., Tonelli, J., 1988. Estimating forest biomass and volume using airborne laser data. *Remote Sens. Environ.* 24 (2), 247–267.
- Nogueira, E.M., Fearnside, P.M., Nelson, B.W., Barbosa, R.I., Keizer, E.W.H., 2008. Estimates of forest biomass in the Brazilian Amazon: new allometric equations and adjustments to biomass from wood-volume inventories. *For. Ecol. Manag.* 256 (11), 1853–1867.
- Nudds, T.D., 1977. Quantifying the vegetative structure of wildlife cover. *Wildl. Soc. Bull.* 113–117.
- Oberbauer, Thomas, 2005. A comparison of estimated historic and current vegetation community structure on Guadalupe Island, Mexico. In: *Proceedings of the Sixth California Islands Symposium*, 6, pp. 143–153.
- Oberbauer, T., Mendoza, L.L., Oliveres, N.C., Deveze, L.B., Duarte, I.G., Morrison, S.A., 2009. Fire on Guadalupe Island reveals some old wounds—and new opportunity. *Fremontia* 37, 3–11.
- O'Hara, K.L., Latham, P.A., Hessburg, P., Smith, B.G., 1996. A structural classification for inland northwest forest vegetation. *West. J. Appl. For.* 11, 97–102.
- Oliver, C.D., 1980. Forest development in North America following major disturbances. *For. Ecol. Manag.* 3, 153–168.
- Parker, G.G., 1995. Structure and Microclimate of Forest Canopies. *Forest Canopy*.
- Pomerleau, F., Breitenmoser, A., Liu, M., Colas, F., Siegwart, R., 2012, September. Noise characterization of depth sensors for surface inspections. In: 2012 2nd international conference on applied robotics for the power industry (CARPI). IEEE, pp. 16–21.
- Popescu, S.C., Wynne, R.H., Scrivani, J.A., 2004. Fusion of small-footprint lidar and multispectral data to estimate plot-level volume and biomass in deciduous and pine forests in Virginia, USA. *For. Sci.* 50 (4), 551–565.
- Ramírez Serrato, N.L., 2014. Índices de vegetación: una herramienta para el monitoreo de esfuerzos de conservación. El caso del Bosque de Ciprés de la Isla Guadalupe. Centro de Investigación Científica y de Educación Superior de Ensenada, Ensenada, Baja California, México.
- Rechsteiner, C., Zellweger, F., Gerber, A., Breiner, F.T., Bollmann, K., 2017. Remotely sensed forest habitat structures improve regional species conservation. *Remote Sensing in Ecology and Conservation* 3 (4), 247–258.
- Rodríguez-Buritica, S., Suding, K., 2013. Interactive effects of temporal and spatial fire characteristics on the population dynamics of a fire-dependent C ypress species. *J. Appl. Ecol.* 50 (4), 929–938.
- Rodríguez-Malagón, M.A., 2006. Diagnóstico del bosque de ciprés de isla Guadalupe a través de imágenes de satélite de alta resolución. Tesis de licenciatura. Universidad Autónoma de Baja California.
- Rogers, D.L., Matheson, A.C., Vargas-Hernández, J.J., Guerra-Santos, J.J., 2006. Genetic conservation of insular populations of Monterey pine (*Pinus radiata* D. Don). *Biodivers. Conserv.* 15 (2), 779–798.
- Rowell, E., Loudermilk, E.L., Hawley, C., Pokswinski, S., Seielstad, C., Queen, L., O'Brien, J.J., Hudak, A.T., Goodrick, S., Hiers, J.K., 2020. Coupling terrestrial laser scanning with 3D fuel biomass sampling for advancing wildland fuels characterization. *For. Ecol. Manag.* 462, 117945.
- Schneider, F.D., Kückenbrink, D., Schaeppman, M.E., Schimel, D.S., Morsdorf, F., 2019. Quantifying 3D structure and occlusion in dense tropical and temperate forests using close-range LIDAR. *Agric. For. Meteorol.* 268, 249–257.
- Seidel, D., Ehbrecht, M., Puettmann, K., 2016. Assessing different components of three-dimensional forest structure with single-scan terrestrial laser scanning: a case study. *For. Ecol. Manag.* 381, 196–208.
- Silva, C.A., Hudak, A.T., Vierling, L.A., Loudermilk, E.L., O'Brien, J.J., Hiers, J.K., Jack, S.B., Gonzalez-Benecke, C., Lee, H., Falkowski, M.J., 2016. Imputation of individual longleaf pine (*Pinus palustris* mill.) tree attributes from field and LIDAR data. *Can. J. Remote Sens.* 42 (5), 554–573.
- Singh, J., Levick, S.R., Guderle, M., Schullius, C., 2020. Moving from plot-based to hillslope-scale assessments of savanna vegetation structure with long-range terrestrial laser scanning (LR-TLS). *Int. J. Appl. Earth Obs. Geoinf.* 90, 102070.
- Srinivasan, S., Popescu, S.C., Eriksson, M., Sheridan, R.D., Ku, N.-W., 2014. Multi-temporal terrestrial laser scanning for modeling tree biomass change. *For. Ecol. Manag.* 318, 304–317.
- Streutker, D.R., Glenn, N.F., 2006. Lidar measurement of sagebrush steppe vegetation heights. *Remote Sens. Environ.* 102 (1–2), 135–145.
- Szostak, M., 2020. Automated land cover Change detection and Forest succession monitoring using LIDAR point clouds and GIS analyses. *Geosciences* 10 (8), 321.
- Tao, S., Guo, Q., Xu, S., Su, Y., Li, Y., Wu, F., 2015. A geometric method for wood-leaf separation using terrestrial and simulated lidar data. *Photogramm. Eng. Remote Sens.* 81 (10), 767–776.
- Van Leeuwen, M., Nieuwenhuis, M., 2010. Retrieval of forest structural parameters using LidAR remote sensing. *Eur. J. For. Res.* 129 (4), 749–770.
- Vera-Ortega, L.A., 2019. Monitoreo de recuperación del Bosque de Ciprés de Isla Guadalupe, por medio del modelado de estructura del dosel, su impacto en la erosión y la hidrología superficial. In: *Centro de Investigación Científica y de Educación Superior de Ensenada, Ensenada, Baja California, México*.
- Vierling, K.T., Vierling, L.A., Gould, W.A., Martinuzzi, S., Clawges, R.M., 2008. Lidar: shedding new light on habitat characterization and modeling. *Front. Ecol. Environ.* 6 (2), 90–98.
- Wan Mohd Jaafar, W.S., Woodhouse, I.H., Silva, C.A., Omar, H., Abdul Maulud, K.N., Hudak, A.T., Klauber, C., Cardil, A., Mohan, M., 2018. Improving individual tree crown delineation and attributes estimation of tropical forests using airborne LidAR data. *Forests* 9 (12), 759.
- Wang, X., Zheng, G., Yun, Z., Xu, Z., Moskal, L.M., Tian, Q., 2020. Characterizing the spatial variations of Forest unlit and shaded components using discrete aerial Lidar. *Remote Sens.* 12 (7), 1071.
- Watt, P.J., Donoghue, D.N.M., 2005. Measuring forest structure with terrestrial laser scanning. *Int. J. Remote Sens.* 26 (7), 1437–1446.
- Yubo, L., Hongyu, H., Liyu, T., Chongcheng, C., Hao, Z., 2019. Tree height and diameter extraction with 3D reconstruction in a Forest based on TLS. *Remote Sensing Technology and Application* 34 (2), 243–252.
- Zhu, X., Skidmore, A.K., Darvishzadeh, R., Niemann, K.O., Liu, J., Shi, Y., Wang, T., 2018. Foliar and woody materials discriminated using terrestrial LidAR in a mixed natural forest. *Int. J. Appl. Earth Obs. Geoinf.* 64, 43–50.